SENSING LOW-VELOCITY IMPACT-INDUCED DELAMINATION IN CARBON FIBER-REINFORCED COMPOSITES THROUGH MEASURING ELECTRICAL RESISTANCE

Robert J. Hart[1], Olesya I. Zhupanska[2], Brandon M. Demerath[1]

[1] Department of Mechanical and Industrial Engineering
The University of Iowa, 3131 Seamans Center, Iowa City, IA 52242
[2] Department of Aerospace and Mechanical Engineering
University of Arizona, 1130 N. Mountain Ave. P.O. Box 210119, Tucson, Arizona 85721

Abstract

In this paper, finite element (FE) models were developed in ABAQUS for studying the influence of low-velocity impact-induced delamination on the 4-probe electrical resistance of carbon fiber-reinforced polymer matrix (CFRP) laminates. The specimens in the current study were 32-ply IM7/977-3 laminates with cross-ply layup. Damage sensing simulations were performed using two methods. In the first method, experimental tests were performed for characterizing the response of the CFRP specimens subjected to low-velocity impact. Computerized tomography (CT) scans were then performed on the damaged specimens in order to assess the internal delamination damage. In the second method, FE models were created in ABAQUS for predicting low-velocity impact-induced delamination using a quasi-static loading approach. Next, both the CT- and simulation-based delaminations were incorporated into 4-probe electrical FE models. A direct current of 10mA was applied to the electrical models in order to determine the influence of the impact-induced delamination on 4-probe electrical resistance using top and oblique measurement planes. For the top measurement plane, source and sensing electrodes were placed in a single line on the top surface of the specimen. For the oblique measurement plane, positive source and sensing electrodes were placed on the top surface, whereas the negative source and sensing electrodes were located on the bottom surface of the specimen. The electrical simulations demonstrated that the impact damage resulted in an increase in electrical resistance. Moreover, as the peak impact load increased, the resistance increased at a nonlinear rate.

Background and Requirements

In the automotive industry, carbon fiber structures are growing in popularity. Where in past decades, these advanced materials were only seen in high-end supercars, in more recent years, carbon fiber-reinforced polymer (CFRP) materials have surfaced in more economical vehicles. CFRP materials provide exceptional mechanical properties and design flexibility at a reduced weight compared to metals. These traits make CFRP composites an attractive choice for fuel- efficient electric and hybrid-electric vehicles. One drawback for CFRP composites and composite laminates is poor impact performance. This weakness has undoubtedly stunted the adoption of CFRP composites in the military ground vehicle industry. At high velocity (i.e. ballistic impact), concentrated impact loads can cause severe damage to CFRP structures. Potentially even more concerning is that low-velocity impact (<200 ft/s) can silently degrade composite material performance during regular use.

In ground vehicle applications, common low-velocity impact events include: road debris (rocks, etc.), maintenance (dropping tools, hitting components with wrenches, etc.), dropping loads (loading/unloading vehicle), and more. These common low-velocity impact events can

lead to severe reduction in structural performance, and in some cases, the damage is not even detectable by the human eye. This type of damage is commonly called Barely Visible Impact Damage (BVID). Low-velocity impact-induced BVID has been correlated with reduced compressive strength [1] and reduced structural integrity. In order to characterize internal damage, advanced imaging techniques have been employed.

Imaging techniques used for characterizing damage in CFRP composites have included: ultrasonic C-scan, infrared thermography, scanning electron microscopy (SEM), computerized tomography (CT) imaging, and others. Ultrasonic C-Scan inspection involves sending ultrasonic pulses into the composite material. Thermography relies on application of a brief heat flow into the composite material. Internal flaws are identified using infrared cameras [2]. SEM produces images of a specimen through the use of a focused beam of electrons that interacts with the atoms in the material. [2,3]. A disadvantage of SEM is that specimens may require significant preparation, such as application of a metallic coating, in order to reflect the electrons properly. CT imaging serves as an excellent alternative for developing 3-D images of the microstructure within a composite material. This technique has been refined over the past several decades for medical applications and in more recent years has been used for illuminating the microstructure of CFRP composites.

Haboub et al. [4] developed an experimental setup for in-situ X-ray tomography during tensile testing and was able to capture matrix cracks that were bridged by continuous fibers. Song [5] utilized CT imaging for quantifying low-velocity impact damage in satin weave carbon-epoxy composites. Demerath [6] performed similar analysis for studying delamination caused by low-velocity impact in IM7/977-3 cross-ply laminates. Experimental characterization of internal damage becomes a time-consuming and expensive process, so some researchers have developed finite element (FE) methods for predicting low-velocity impact damage in CFRP laminates.

De Moura and Marques [1] developed a FE framework for predicting low-velocity impact – induced delamination in CFRP composites. The FE model was created in ABAQUS and was based around a special 8-node shell element (S8R) that guarantees interlaminar shear stress continuity between differently oriented layers. The FE model assumed negligible transverse normal stress (through thickness direction) and quasi-static stress analysis. The quasi-static analysis saved computational cost and was justified in that delamination can be predicted using only maximum impact force (i.e. does not require the dynamic force history). The shell element further improved computational costs, because it only required one element per layer thickness and allowed stress calculation at multiple points through the element thickness. The interlaminar shear stresses were then used in evaluating delaminations in the composite. The predicted delaminations had the correct shape and orientation compared to experiments, but the overall delaminated area was only marginally accurate. In order to better predict the delaminated area, progressive damage models are needed. While prediction of impact damage is of interest to researchers and designers, field engineers and technicians require methods for sensing and measuring impact damage. One popular damage-sensing method in development is based on the inherent electrical properties of carbon fibers.

Numerous experimental studies have proved that monitoring changes in electrical resistance can be an effective technique for damage sensing of CFRP composites. In the four-probe resistance method [7–12], current source and measurement probes are arranged along a single line on the surface of the composite which enables the resistance to be calculated through Ohm's law. Delamination increases through thickness resistivity due to a reduction in contact between the fibers in adjacent lamina. Four distinct measurement planes are used to capture these damage mechanisms [10,11]. The top and bottom surface measurement planes

provide excellent sensitivity to fiber breakage whereas the through thickness measurement plane provides the most sensitive response to delamination and fiber-matrix debonding. The oblique plane (i.e.: through the thickness at an oblique angle) measurement is sensitive to all three damage modes [12].

McAndrew and Zhupanska [10] studied the influence of low-velocity impact on electrical resistance in AS4/3501-6 CFRP laminates with layup arrangements of $[0/45/-45/90]_{2s}$ and $[0/45/-45/90]_{4s}$. The specimens were square 152.4mm x 152.4mm with thicknesses of 2.25mm and 4.5mm, respectively. Four-probe resistance measurements were observed through the top and oblique measurement planes. For a single impact event, the oblique resistance was found to be more sensitive to impact damage compared to the top surface resistance. The top resistance measurement failed to capture the impact damage in several of the specimens, even with visible impact damage. Although in this study the resistance method did show limited success in identifying impact damage, the measurements were not sensitive enough to distinguish between the magnitudes of impact energy applied to the specimen.

In this paper, low-velocity impact-induced delaminations were characterized using two methods. First, impact experiments were performed and CT scans were constructed for the damaged specimens. The CT image-based delaminations were then integrated into electrical damage sensing models to observe the influence of the delamination on electrical resistance. In the second method, data from the impact experiments were used to develop predictive FE impact models following the work of Moura [1]. These simulation-based delamination predictions were also integrated into the damage sensing models and the results were compared to the previous CT image-based results.

Experimental Methods

The experimental techniques in this paper were aimed at characterizing low-velocity impact damage in CFRP laminates through CT imaging. First, low velocity impact characterization was completed. Specimens were then analyzed via CT imaging in order to observe the internal damage.

Description of Specimens

The specimens tested were 32-ply cross-ply CFRP laminates in the symmetric configuration: IM7/977-3 $[0/90]_{8S}$. The specimens were laminated using prepeg tape consisting of aerospace grade IM7 carbon fibers [13] and 977-3 toughened epoxy resin [14]. The laminated thickness was 4.30mm. The individual specimens were cut from larger sheets to the size 152.4 x 152.4mm using a CNC water-jet.

Low-Velocity Impact Testing

Low-velocity impact characterization was performed using an Instron 8200 Dynatup low-velocity impact tester. The Instron 8200 is suited primarily for plastic and composite materials and is capable of a maximum drop height of 1 meter, maximum impact velocity of 4.4 m/s, and maximum impact energy of 132.8 Joules. The drop height was measured as the distance between the top surface of the clamped specimen and the bottom of the striker head, with the drop weight carriage at the set position. The striker consisted of a load cell, or tup, and tup insert that covers the outside of the load cell and comes in direct contact with the test specimen. Specimens were tested under 3 different loading conditions. First, three specimens were impacted with a 12.7mm hemispherical-tipped tup insert at an impact velocity of 1.72 m/s. Next,

three additional specimens were impacted with the same tup insert at a slightly higher velocity of 2.10 m/s. Finally, three more specimens were tested using a 12.7mm flat-ended tup insert at the same velocity of 2.10 m/s. The impact energies were 18.93, 28.29, and 28.42 J, respectively. The impact energy for the third test group was only marginally higher than the second test group, but for convenience, in this paper, the three test groups were labeled as low, intermediate, and highest impact energy. The specimens were assigned the labels 32-X-Low, 32-X-Int, and 32-X-High, respectively. Throughout this paper, the reported values for impact velocity, peak load, and impact energy were averaged for each set of three specimens.

CT Imaging

In order to observe the interior microstructure of the specimens, CT scans were conducted courtesy of Schneider Electric in Cedar Rapids, IA. The CFRP specimens were scanned using a Zeiss METROTOM 1500 computed tomography (CT) system. The METROTOM 1500 can produce voxel (volumetric pixel) resolutions ranging from 5 µm to 400 µm and can scan objects as large as a 300 mm by 300 mm cylinder [6]. The CT scans were reconstructed into 3D image stacks using VGStudio MAX by the CT Analyst at Schneider Electric and further processed using myVGL Viewer by Hart and Demerath.

Finite Element Modeling

There were two primary objectives in the FE modeling work. The first objective was to develop quasi-static FE models for predicting low-velocity impact-induced delamination in CFRP laminates. The second objective was to integrate both the CT image-based and FE prediction-based delamination patterns into electrical resistance damage sensing FE models. For more detailed explanation of the finite element procedures, refer to the Hart thesis [15].

Delamination Predictions Using Quasi-Static Impact Models

Following the methodology of Moura et al [1], low-velocity impact models were developed in ABAQUS for the purpose of predicting damage in carbon-epoxy composites. The geometry was modeled to follow the experimental test fixture and boundary conditions in Figure 1. The geometry was meshed using the 8-node S8R shell element.

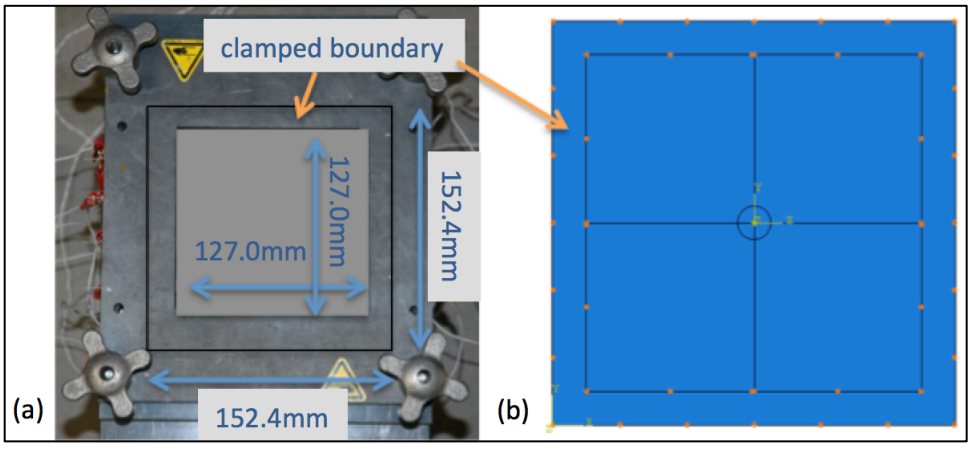

Figure 1: (a) Low-velocity impact test fixture and (b) FE boundary conditions and loads for quasi-static impact models.

With the S8R element, shear stress continuity was maintained between adjacent plies. For delamination prediction, a quasi-static loading approach was utilized (i.e. damage is predicted using only the peak impact load and was not rate-dependent). A two-step failure criterion was utilized for analyzing failure on a ply-by-ply basis. Moura et al [1] developed the failure criteria by using a combination of the methods from Tsai and Wu, Hashin, Choi, and Becker [16–19] as well as information gathered from experimental work. Based on the results of Choi [19], delamination occurs at the interface between plies with different fiber orientations and is caused by matrix cracking within the adjacent plies. The first step in the failure analysis was to predict the presence of matrix cracks within the plies using the following failure criterion:

$$\left(\frac{\sigma_2}{Y_{t,c}}\right)^2 + \left(\frac{\tau_{23}}{S_i}\right)^2 = 1 \qquad (1)$$

where σ_2 is the second principle stress, τ_{23} shear stress in 2-3 plane, $Y_{t,c}$ is the material strength in the 2-direction (tension or compression depending on the sign of σ_2), and S_i is the material shear strength. If matrix cracking was predicted within a ply, then the second step was to perform delamination analysis on the adjacent ply. For interior plies, the delamination analysis was performed at the interface between the two differently oriented plies using stresses on the side of the lower ply. For the lowest ply (furthest from the impacted surface), the delamination was performed using stresses at the interface on the side of the upper adjacent ply. The delamination was predicted using the following expression:

$$\left(\frac{|\sigma_1^*|}{X_{t,c}}\right) + \left(\frac{\sigma_1^*}{X_{t,c}}\right)^2 + \left(\frac{|\sigma_2^*|}{Y_{t,c}}\right) + \left(\frac{\sigma_2^*}{Y_{t,c}}\right)^2 + \left(\frac{2|\sigma_1^*\sigma_2^*|}{X_{t,c}Y_{t,c}}\right) + \left(\frac{|\tau_{13}|_n}{S_i}\right) + \left(\frac{\tau_{13_n}}{S_i}\right)^2 = 1 \qquad (2)$$

where σ_1^* and σ_2^* are principal stresses, τ_{13} is the transverse shear stress in 1-3 plane, $X_{t,c}$ is the material strength in tension/compression in the 1-direction. The difference between the expression (2) and the delamination equation of Moura et al [1] was that in the expression (2), the σ_1^* was compared to the material strength in the fiber direction ($X_{t,c}$), following the Hashin criteria [17]. The peak impact load was applied to each model at the center of the specimen and the load was appropriately distributed depending on the type of impact striker used in the experiment. For more information on stress concentration for each striker tip see the paper from Demerath [6].

The next step in the modeling process was to compile the necessary mechanical properties for the FE analysis. For the S8R shell element with orthotropic material properties, ABAQUS required the following parameters: density (kg/m^3), elastic modulus (E_{11} and E_{22} in Pa), Poisson's ratio (ν_{12}), and shear modulus (G_{12}, G_{13}, and G_{23} in Pa). Generally, only constituent material properties (fiber/matrix) are published in material datasheets, thus in order to determine the appropriate composite properties, basic theory was employed. Knowing the proportions of fibers and matrix in a given composite, the mechanical properties can be approximated using the properties of the individual constituents and a set of special relations, generally referred to as the "rule of mixtures" [20].The fiber and matrix constituent properties were gathered from material datasheets [13,14,21–23] and are compiled in Table I.

Table I: Quasi-Static Impact Modeling Parameters

Constituent Properties	
Material Property	**IM7/977-3**
Fiber % / Matrix%	78%/22%
ρf / ρm [kg/m3]	1780/1310
Ef / Em [Pa]	2.76E+11/3.52E+09
vf / vm	0.3/0.384
Composite Properties	
Material Property	**IM7/977-3**
ρ [kg/m3]	1676.6
E11 [Pa]	2.161E+11
E22 [Pa]	1.530E+10
v12	0.318
G12 [Pa]	5.540E+09
G13 [Pa]	5.540E+09
G23 [Pa]	5.220E+09
Xt [Pa]	2.723E+09
Xc [Pa]	1.689E+09
Yt [Pa]	1.11E+08
Yc [Pa]	1.11E+08
Si [Pa]	1.28E+08

Four Probe Electrical Finite Element Models

In this paper, the damage sensing simulations were performed using a traditional four-probe electrical resistance configuration, shown in Figure 2. The electrodes were made from 22-gage copper wire and were assigned equal spacing of 30mm center-to-center, resulting in a total distance of 90mm center-to-center between the positive and negative current source electrodes. A direct current of 10mA was applied as a positive current flux onto the left source electrode and a negative current flux on the right source electrode. For the top resistance test, the electrodes 1 and 4 (see Figure 2) were used as source electrodes and electrodes 2 and 3 were used for sensing the resistance. For the oblique resistance test, electrodes 1 and 8 were source electrodes and electrodes 2 and 7 were used for sensing the specimen resistance. The specimens were modeled using standard linear, thermal-electric hexagonal elements. The

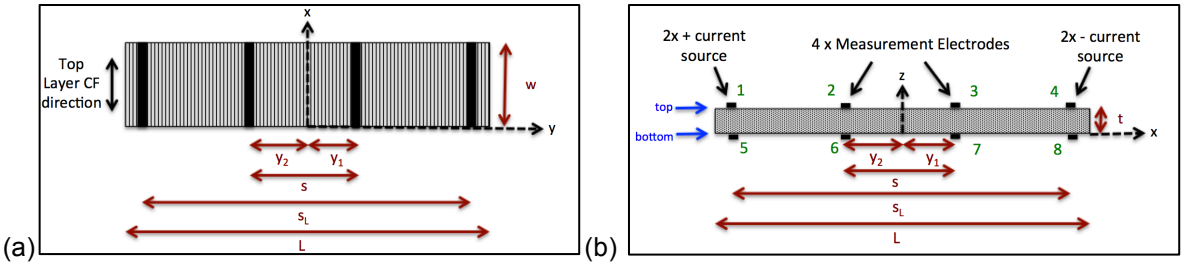

Figure 2: (a) Top and (b) side views of schematic of 4-probe resistance method. For top resistance measurement, electrodes 1,2,3,4 are utilized. For oblique resistance measurement, electrodes 1,2,7,8 are utilized. Note: in (a) the specimen was cropped to better fit the page and appears as an oblong rectangle. In the tests, the specimen was square with L=w=152.4mm.

composite material was modeled as an orthotropic material with no distinction between the fibers and matrix. The electrical conductivity in the fiber, transverse, and through thickness directions were: 29330, 1.61 and 0.287 S/m, respectively [15]. The conductivity of copper was 5.96 E7 S/m.

Integration of Delamination Predictions into Electrical Resistance Sensing Models

In order to integrate the delamination damage into the electrical FE models, the CT- and FE-based delamination was discretized into a grid and then copied onto the mesh in the ABAQUS electrical damage sensing FE Models. Once the delamination was integrated into the ABAQUAS FE models, top and oblique resistance simulations were performed for each damaged specimen. In the current paper, the low-velocity impact was not considered especially severe and was performed at such energy that only barely visible impact damage was sustained. For such a scenario, it is reasonable to assume there may be some fiber to fiber contact occurring across the delaminated interface, which would allow current to flow across the interface, but at a rate less than in an undamaged specimen. In this case, the through-thickness conductivity of the damaged elements was appropriately reduced following the previous work of Pyrzanoski et al [24]. For the delaminated elements in the current study, the electrical conductivity in the through-thickness direction was reduced by a factor of two in order to represent of the reduction of contact between the adjacent plies.

Results

CT Imaging

The 3-D CT scans were deconstructed into 2-D image slices and extracted each interface between plies of different fiber orientations. In the symmetric, 32-ply specimens, this resulted in 30 interface regions with potential for delamination damage. Interfaces were numbered 1-30 from top to bottom. The original CT image files were in gray scale, and it was difficult to discern damage from undamaged material. In order to better discern between the damage and undamaged regions, the gray values were adjusted such that the normal, undamaged CFRP specimen was colored blue, and the damaged (or delaminated) regions were yellow, as shown in Figure 3 (a). The delaminated areas were then identified and measured so that they could be incorporated into the damage sensing models.

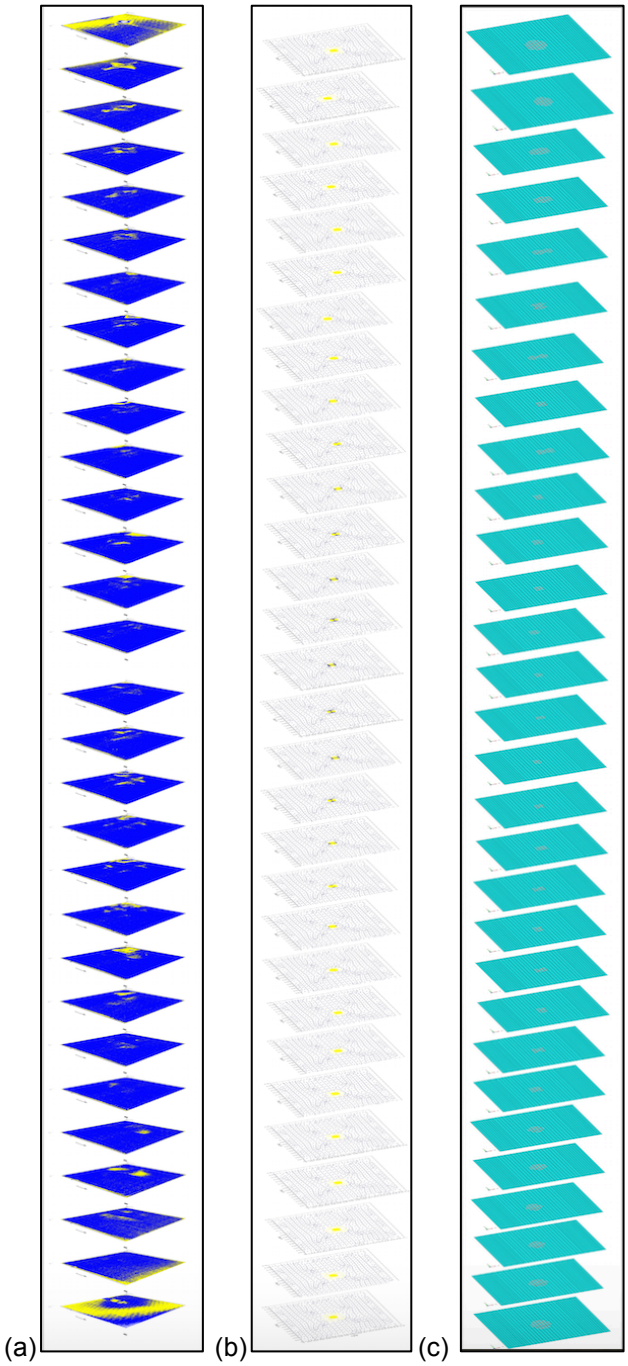

Figure 3: Image stack of 30 interfaces for specimen 32-X-Low from (a) CT Scan, (b) Matlab damage prediction, and (c) ABAQUS electrical FE model.

FE Delamination Predictions

In order to analyze the 32-X specimens and validate the FE predictions, the delamination plots were compared to CT image results at a two interfaces, shown in Figures 4-5. These

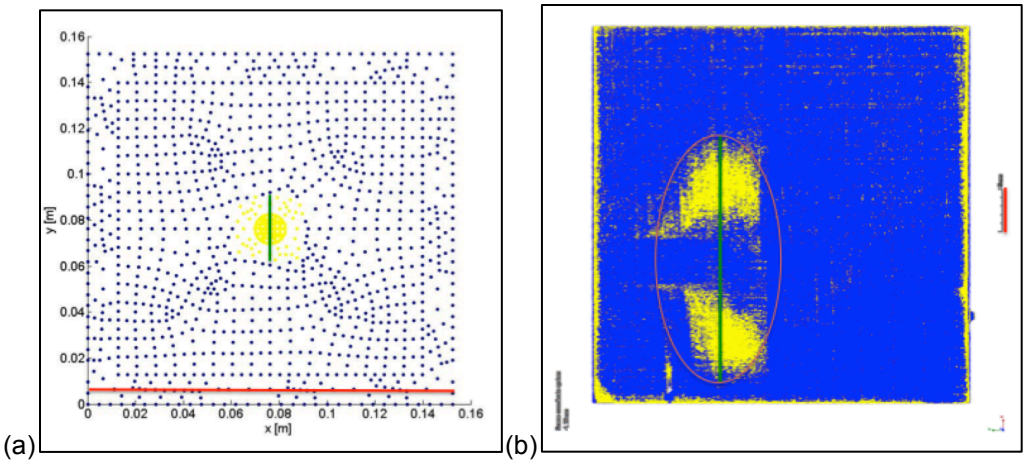

Figure 4: Comparison of (a) FE delamination prediction and (b) CT image [6] *at interface 27 for 32-X-Low specimen. (Note: FE plot in part (a) is full 152.4mm x 152.4mm specimen, whereas the CT image in part (b) is cropped to show detail in only a 45 mm x 45 mm section).*

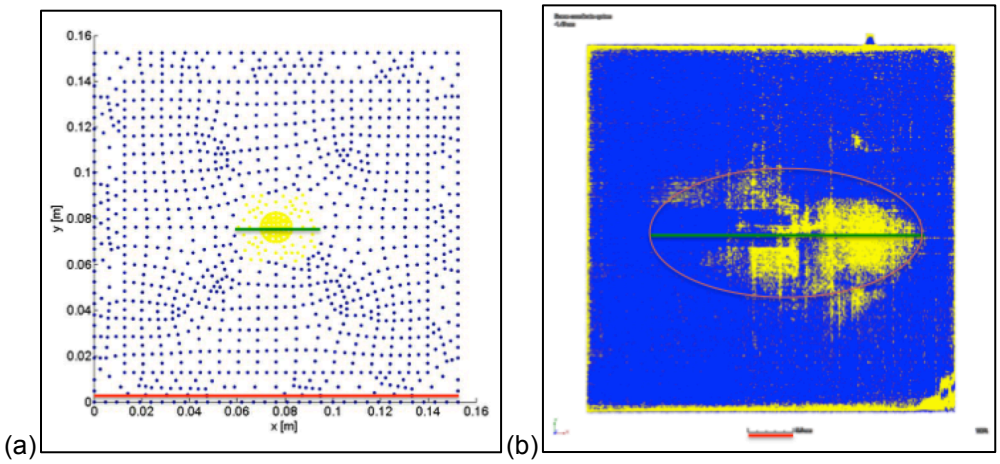

Figure 5: Comparison of (a) FE delamination prediction and (b) CT image [6] *at interface 26 for 32-X-Int specimen. (Note: FE plot in part (a) is full 152.4mm x 152.4mm specimen, whereas the CT image in part (b) is cropped to show detail in only a 45 mm x 45 mm section).*

interfaces were selected, because of two criteria: (i) these were identified as the most severely delaminated interfaces via CT scans and (ii) there was minimal shadowing present in the CT data. One clear disparity between the FE predictions and CT image results was that for the FE predictions, the maximum length of the delaminated region was at the lowest interface 30, where as for the experimental CT specimens, the maximum delaminated interface was at interface 27 for specimen 32-X-Low and interface 26 for 32-X-Int. This discrepancy was expected, however, because the quasi-static FE models did not take progressive failure into account, therefore the delamination was based only on static stress values alone. Based on beam theory, stresses are maximum at either the top or bottom surface, which supports the prediction of maximum delamination at the lowest interface 30. For further investigation, the

maximum length of the delamination major axis was compared between the FE models and CT scans. The CT scan and FE prediction differed by only 0.1mm, or 0.4%, for 32-X-Low at interface 27. For 32-X-Int at interface 26, the difference was only 2.2mm, or 6.2%. This deviation was considered acceptable due to the assumptions of the quasi-static method and the relatively large amount of noise/shadowing present in the CT scans. Once the delamination was characterized by CT and FE methods, the next step was to incorporate the damage into the electrical FE models to see the influence of damage on electrical resistance.

Comparison of Influence CT and FE Delamination on Electrical Resistance

Four-probe electrical simulations were conducted on specimens subjected to three different impact loading conditions. For the 32-X-Low specimen, the top and oblique resistance increased by 0.157% and 0.242%, respectively. For the 32-X-Int specimen, top and oblique resistance increased by 0.258% and 0.433%, respectively. Finally, for the 32-X-High specimen, top and oblique resistance increased by 0.558% and 0.711%, respectively. These results indicated that as impact energy (peak load) increased, the resistance continued to escalate due to an increase in the delamination damage. Peak impact load for the low, intermediate, and high-energy tests were 7786 N, 9253 N, and 11748 N, respectively. From the low to high-energy tests, the peak impact load increased by a factor of 1.5. This increase in peak load was coupled with an even more dramatic change in resistance. The changes in top and oblique resistance due to the impact increased by a factor of approximately 3 when comparing the low and high-

Table II: FE Simulation Results for Top and Oblique Resistance

Impact Description	FE-Based Delamination		CT-Based Delamination	
	Top Resistance [Ohm]	Oblique Resistance [Ohm]	Top Resistance [Ohm]	Oblique Resistance [Ohm]
None	2.948E-02	6.297E-01	2.948E-02	6.297E-01
Low Energy	2.953E-02	6.312E-01	2.949E-02	6.308E-01
Change	**4.62E-05**	**1.52E-03**	**1.00E-05**	**1.10E-03**
% Change	**0.16%**	**0.24%**	**0.03%**	**0.17%**
Int Energy	2.956E-02	6.324E-01	2.949E-02	6.309E-01
Change	**7.61E-05**	**2.73E-03**	**1.30E-05**	**1.16E-03**
% Change	**0.26%**	**0.43%**	**0.04%**	**0.18%**
High Energy	2.960E-02	6.340E-01	N/A	N/A
Change	**1.65E-04**	**4.48E-03**	**N/A**	**N/A**
% Change	**0.56%**	**0.71%**	**N/A**	**N/A**

energy simulations. This result indicates that there may be a non-linear correlation between peak impact load and electrical resistance. The overall sensitivity of the resistance to damage was not especially significant, however, as the resistance changed by less than 1% for all simulations. This modest increase in resistance follows some previous experimental results for similar CFRP composites [10]. Additional work in the Hart thesis [15] suggested that in order to improve sensitivity to damage, the electrodes need to be spaced closer than the overall size of the damage. In the current paper, electrode spacing (30mm) was slightly greater than the largest delaminations in Figures 4 and 5. In order to improve sensitivity, future work should focus on optimizing the electrode spacing to achieve a desired sensitivity while still maximizing coverage volume.

Summary and Next Steps

In this paper, FE models were leveraged for observing the influence of low-velocity impact-induced delamination on the 4-probe electrical resistance of CFRP laminates. Experimental tests were performed for characterizing the response of the CFRP specimens subjected to low-velocity impact. Next, CT scans were constructed for the damaged specimens in order to assess the presence of internal delaminations. FE models were then created for predicting low-velocity impact-induced delamination using a quasi-static loading approach. The CT- and FE-based delaminations were then incorporated into 4-probe electrical FE models to analyze damage sensing trends. The electrical simulations demonstrated that the impact resulted in an increase in electrical resistance. Moreover, as the peak impact load increased, the resistance increased at a nonlinear rate. Future work should focus on optimizing electrode placement to improve sensitivity to damage as well as to analyze the damage sensing capabilities of more complex geometries and curved surfaces.

Acknowledgements

Robert Hart would like to extend his sincere gratitude to the SPE Foundation for support through the 2016-2017 Dr. Jackie Rehkopf Scholarship, which enabled the completion of this PhD research work.

References

[1] de Moura MFSF De, Marques AT. Prediction of low velocity impact damage in carbon - epoxy laminates. Compos Part A 2002;33:361–8.

[2] Ashrafi B, Diez-Pascual AM, Johnson L, Genest M, Hind S, Martinez-Rubi Y, et al. Processing and properties of PEEK/glass fiber laminates: Effect of addition of single-walled carbon nanotubes. Compos Part A Appl Sci Manuf 2012;43:1267–79. doi:10.1016/j.compositesa.2012.02.022.

[3] Chang C-Y, Phillips EM, Liang R, Tozer SW, Wang B, Zhang C, et al. Alignment and properties of carbon nanotube buckypaper/liquid crystalline polymer composites. J Appl Polym Sci 2012:1360–8. doi:10.1002/app.38209.

[4] Haboub A, Bale H a., Nasiatka JR, Cox BN, Marshall DB, Ritchie RO, et al. Tensile testing of materials at high temperatures above 1700 °C with in situ synchrotron X-ray micro-tomography. Rev Sci Instrum 2014;85:83702. doi:10.1063/1.4892437.

[5] Song C. Low velocity impact testing and computed tomography damage evaluation of layered textile composite. 2014.

[6] Demerath BM. LOW VELOCITY IMPACT DAMAGE ASSESSMENT IN IM7/977-3 CROSS-PLY COMPOSITES USING 3D COMPUTED TOMOGRAPHY. 2015.

[7] Wang S, Chung DDL, Chung JH. Impact damage of carbon fiber polymer – matrix composites , studied by electrical resistance measurement. Compos Part A 2005;36:1707–15.

[8] Wang S, Chung DDL. Self-sensing of damage in carbon fiber polymer-matrix composite by measurement of the electrical resistance or potential away from the damaged region. J Mater Sci 2005;40:6463–72.

[9] Ceysson O, Salvia M, Vincent L. Damage Mechanisms Characterisation of Carbon Fibre / Epoxy Composite Laminates by both Electrical Resistance Measurements and Acoustic Emission Analysis. Scr Mater 1996;34:1273–80.

[10] Mcandrew J, Zhupanska OI. Experimental Assessment of Single and Cumulative Impact Damage in Carbon Fiber Polymer Matrix Composites Using Electrical Resistance Measurements. J Multifunct Compos 2014;2:79–91.

[11] Mcandrew J. Impact damage assessment in CFRP composites using 1D electrical resistance technique 2010:52242.

[12] Chung DDL. Damage detection using self-sensing concepts. Proc IMechE 2007;221:509–20.

[13] Hexcel. HexTow ® IM7 2015.

[14] CYTEC. CYCOM ® 977- 3 EPOX Y RESIN SY S TEM CYCOM ® 977-3 Epoxy Resin System 2015.

[15] Hart RJ. ELECTRICAL RESISTANCE BASED DAMAGE MODELING OF MULTIFUNCTIONAL CARBON FIBER REINFORCED POLYMER MATRIX COMPOSITES. University of Iowa, 2017.

[16] Tsai SW, Wu EM. A General Theory of Strength for Anisotropic Materials. J Compos Mater 1971;5:58–80.

[17] Hashin Z. Failure Criteria for Unidirectional FibreComposites. J Appl Mech 1980;47:329–34.

[18] Becker W. Mathematical simulation of external and internal damage due to low velocity impact. Trans Eng Sci 1994;4:2–8.

[19] Choi HY, Chang F-K. A Model for Predicting Damage in Graphite/Epoxy Laminated Composites Resulting from Low-Velocity Point Impact. J Compos Mater 1992;26:2134–69.

[20] Jones RM. Mechanics of Composite Materials. 1998.

[21] Hexcel. HexTow ® AS4. Mater Datasheet 2015:2.

[22] Cytec. Cycom 977-2 Epoxy Resin System -Technical Data Sheet. Cytec - Eng Mater 2012:1–4. http://www.cemselectorguide.com/pdf/CYCOM_977-2_031912.pdf.

[23] Hexcel. 3501-6 Epoxy Matrix. Mater Datasheet 1998:36–9.

[24] Pyrzanowski P, Olzak M. Numerical modelling of resistance changes in symmetric CFRP composite under the influence of structure damage. Compos Sci Technol 2013;88:99–105. doi:10.1016/j.compscitech.2013.08.023.